

EHF based Heatwave Identification and its Impact on Urban Heat Island Intensity: A Case Study of an Indian City

Shikhar Saxena¹, Sonam Agrawal², Debolina Basu³

¹ Geographic Information System (GIS) Cell, Motilal Nehru National Institute of Technology Allahabad, Prayagraj (U.P.) - 211004, India – shikhar.2022rgi01@mnnit.ac.in

² Geographic Information System (GIS) Cell, Motilal Nehru National Institute of Technology Allahabad, Prayagraj (U.P.) - 211004, India – sonam@mnnit.ac.in

³ Department of Civil Engineering, Motilal Nehru National Institute of Technology Allahabad, Prayagraj (U.P.) - 211004, India – basud@mnnit.ac.in

Keywords: Excess Heat Factor, UHI Intensity, MODIS, ERA-5 Land

Abstract

In the Indian subcontinent, the heatwaves occur mainly during the summer months from April to June. This heatwave becomes more severe when accompanied by higher summer temperatures in the country. Excess Heat Factor (EHF) is a metric used to identify heatwaves. This study identifies the heatwave using EHF and its relationship with UHI intensity in pre, post, and during heatwave event. The results show a heatwave event in the area from 10-16 June 2023 with positive EHF values. The values range from 0.433087-5.277442 during the heatwave event. To establish the link between the positive EHF value and UHI intensity, the variation of UHI intensity is monitored using MODIS data. The findings indicated that during the heatwave event, the UHI intensity and its extent grew with an increase in temperature of 2°C in the daytime and slight changes in the nighttime. This result is also validated by plotting the variation of UHI intensity using ERA-5 Land data on the grid point of the weather station (29.5°N, 79.5°E), which ranges between 0.504764 – 0.633209 during the pre-heatwave event. The intensity value kept on increasing as the heatwave event approached and reached the maximum magnitude of 0.70384 during the heatwave event. As the event finishes, intensity values decrease to 0.147939 post heatwave event. The findings provide an understanding of localized interaction of UHI intensity and the heatwave which is identified using the EHF factor.

1. Introduction

The Urban Heat Island (UHI) effect has impacted many regions worldwide for several decades. The UHI can be expressed as a phenomenon of elevated temperatures within the cities compared to their rural surroundings (He et al., 2021). Due to this, many extreme weather events, like floods, droughts, cyclones, heatwaves, etc., are causing much damage to the people and environment. These extreme climate events are happening at higher frequencies globally. This increase in the frequency of events globally is due to the substantial rise in global temperatures. The global annual mean temperature has been increased by 1°C to 2°C (IPCC, 2022). This highlights the necessity for identifying and understanding the variation of extreme temperature events, i.e., heatwaves (Mamgain et al., 2023). Heatwaves are generally defined as prolonged periods of excessive hot weather. Among the South Asian countries, India is highly vulnerable to heatwave events due to its complicated landscape, dense population, and urbanization (Goyal et al., 2023).

A study conducted on 2022 heatwave events in India, using the method of event attributions, states that the probability of occurrence of such heatwave events had increased by a factor of 30 for the year 2022 and will happen more frequently as well as severely in the future (Zachariah et al., 2022). The increasing trend in the heatwaves and their severity in India in recent years and in the near future is also documented (Rao et al., 2023; Rohini et al., 2016). Heatwaves usually occur over larger areas, but this problem is more prominent in urban areas. The magnanimity of this problem could be understood by the United

Nations report, which states that urban dwellers are projected to account for 68% of the global population by 2050 (UN Habitat, 2022).

Cities accumulate more heat than rural areas. The metropolitan areas are accruing more heat during the day, increasing the intensity of heatwaves in the cities. The daytime increase in the local temperatures significantly reduces the drop in nighttime temperature. This creates serious inconvenience in the case of "tropical" ($> 20^{\circ}$ C) and "torrid" nights ($> 25^{\circ}$ C) (Tan et al., 2010). This results in persistent heat stress during the day and nighttime (Arellano and Roca, 2022). It is therefore crucial to study heatwave characteristics and their impact on regional warming levels in the cities both day and night time.

Various heatwave metrics have been used in the literature to study heatwave characteristics, ranging from temperature only to thermal composite metrics incorporating variations in temperature and other factors (Xu et al., 2016). Besides this variation, the intensity and the duration of heatwave vary according to the definition (Anderson & Bell, 2011; Ma et al., 2015). This absence of a universal heatwave definition can be challenging for government agencies and emergency response services to understand easily. To address this, the Australian Bureau of Meteorology (BOM) developed a metric called the "Excess Heat Factor" (EHF) that can be applied consistently across different locations to indicate heatwave severity and intensity (Nairn & Fawcett, 2014). According to this metric, heatwave conditions occur in an area where there is a significant temperature anomaly (both short-term and long-term) specific to that location. The EHF metric has been used in several

studies in Australia (Hatvani-Kovacs et al., 2016; Scalley et al., 2015) and elsewhere (Urban et al., 2017; Wang et al., 2018). These studies suggest that EHF is a valuable indicator of heat-health impacts and, therefore, a potential heat warning indicator of heat-related occupational injuries and illnesses (Sy et al., 2022; Zhang et al., 2023). These studies also highlighted the need for effective heatwave management strategies. These management plans have been implemented successfully when there is a proper understanding of whether there is any synergistic relationship between UHI and heatwaves. Most of the studies carried out in the context of heatwaves provide information about heatwaves but on the other hand, despite the effectiveness of the EHF metric in heatwave estimation, this metric has yet to be used to evaluate the heatwaves in India. Therefore, this study aims to identify the heatwave using the EHF metric and to investigate the spatio-temporal nocturnal and diurnal variation in UHI intensity.

2. Study Area

Farrukhabad is a city in the state of Uttar Pradesh, India. It lies between $26^{\circ} 46' N$ to $27^{\circ} 43' N$ and $79^{\circ} 7' E$ to $80^{\circ} 2' E$. This city is on the banks of the river Ganges. As per the 2011 census, Farrukhabad had a population of 276,581, along with Fatehgarh (Khanna, 2023). The hottest month of the year is June, with temperatures increasing to $42^{\circ}C$. The district is bounded by Badaun and Shahjahanpur on the north, Hardoi on the east, Kannauj on the south, and Etah and Mainpuri on the west. The total area of district Farrukhabad is 2,28,830 Hectares. Farrukhabad is famous for its cloth printing, textile printing, block printing, and Jari Jardoji industry.

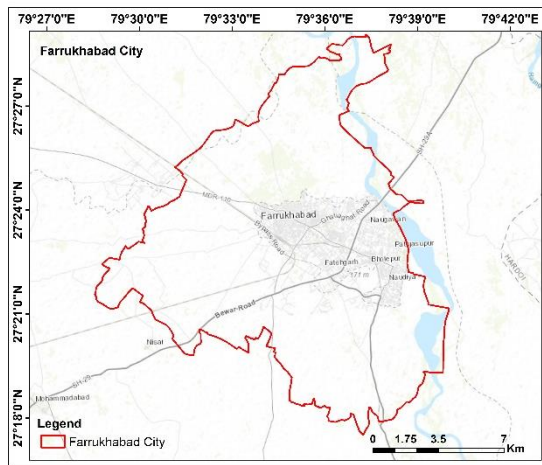


Figure 1. Study Area

3. Material and Methods

3.1 Data Used

In this study, the daily gridded temperature data (maximum and minimum) was collected from 1994-2023 for a weather station ($29.5^{\circ} N$, $79.5^{\circ} E$) located in Farrukhabad, Uttar Pradesh. This data is available at the Data Supply Portal of the Indian Meteorological Department. This dataset is available at a spatial resolution of $1^{\circ} \times 1^{\circ}$ ($111.1 \text{ km} \times 111.1 \text{ km}$). This data is used to calculate the EHF values.

Another dataset applied in this study is the LST product of the MODIS sensor onboard Tera satellites. It measures the radiation from the earth's surfaces in 36 broad spectral bands between 0.4 and $14.4 \mu\text{m}$. The Aqua satellite passes around 13:30 local solar

time over the study location during the daytime. In the nighttime, it passes around 10:30 local solar time. The present study considered a global daily LST data (MOD11A1) of 1 km spatial resolution.

3.2 Generation of LST images from MODIS data

In this study, the daily LST data for the peak heatwave month of June as per IMD for the year 2023 is extracted using Google Earth Engine (GEE) for the region. MODIS data is used to extract this data, but there are some missing dates on which the data is unavailable or missing in this region during heatwave days within the month. MODIS Aqua product is accessible from the collection ("MODIS/061/MOD11A1"). This product contains both the daytime ("LST_Day_1km") and nighttime data ("LST_Night_1km"). After importing the collection, the start and end dates are mentioned to extract the data. To obtain the final LST image, the available date image must be multiplied by the scaling factor of 0.02 to get the image of LST on the Kelvin scale. To convert the image to a degree Celsius scale, 273.15 is subtracted from them. The final LST image is downloaded into the local machine and used for further processing.

3.3 Computation of UHI intensity

In this study, the UHI intensity is estimated using the normalized UHI intensity method, which is given by the equation

$$UHI = \frac{LST - LST_{mean}}{LST_{sd}} \quad (1)$$

where LST is the value of LST in the image, and LST_{mean} and LST_{sd} are the normalized LST mean and standard deviation values calculated from all the images, respectively.

3.4 Excess Heat Factor (EHF) Calculation

EHF is a metric that is used to measure the occurrence of extreme heat events. This metric accounts for maximum temperature, the duration of the event, and severity. EHF was introduced by Narin and Fawcett (Nairn & Fawcett, 2013). This metric is a combination of two excessive heat indices, namely Excess Heat (EHI_{sig}) and Heat Stress (EHI_{accl}). Excess Heat (EHI_{sig}) is usually the heat arising in the daytime, which is not sufficiently discharged overnight due to high overnight temperatures. This index is defined as

$$EHI_{sig} = \frac{T_i + T_{i+1} + T_{i+2}}{3} - T_{95} \quad (2)$$

where T_i is the Daily Mean Temperature (DMT) on the day i and T_{95} is the 95th percentile of DMT for the reference period 1994-2023. DMT is defined as

$$T = \frac{T_{max} + T_{min}}{2} \quad (3)$$

The Heat Stress (EHI_{accl}) arises from a period where the temperature is warmer, on average than in the recent past. Maximum and minimum temperatures are averaged over three days and the previous 30 days to characterize this heat stress. This index is defined as

$$EHI_{accl} = \left(\frac{T_i + T_{i+1} + T_{i+2}}{3} \right) - \left(\frac{T_{i-1} + \dots + T_{i-30}}{30} \right) \quad (4)$$

where $\left(\frac{T_{i-1} + \dots + T_{i-30}}{30}\right)$ is the recent past 30 days mean temperature from day i .

The combined effect of the Excess Heat (EHI_{sig}) and Heat Stress (EHI_{accl}) which provides a comparative measure of the intensity, load, duration, and spatial variation of heatwave events. Heatwave conditions exist when EHF values are positive. EHF is defined as

$$\text{EHF} = \max(0, \text{EHI}_{\text{sig}}) \times \max(1, \text{EHI}_{\text{accl}}) \quad (5)$$

EHF is used to identify the heatwave days in the present study. Positive value of EHI_{sig} define heatwave-like conditions for i^{th} day, if $\left(\frac{T_i + T_{i+1} + T_{i+2}}{3}\right) > T_{95}$ for at least three consecutive days, then these days are considered as heatwave.

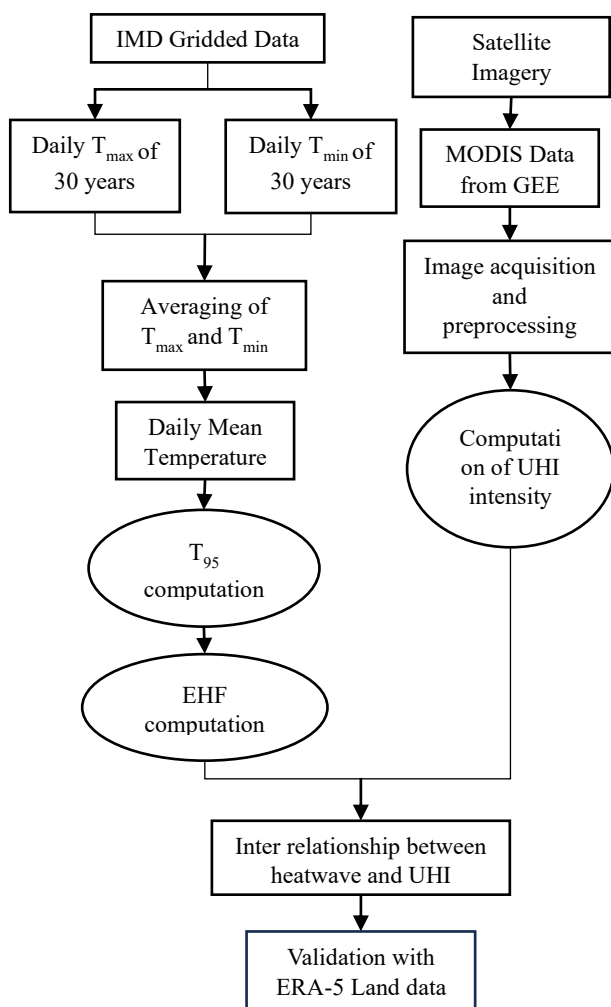


Figure 2. Methodology flowchart

4. Result and Discussion

4.1 EHF calculation

The EHF values are calculated for the hottest summer month, i.e., June. The values are calculated on the daily temperature data acquired by IMD. The EHF values are supposed to be positive for three days to confirm the heatwave-like scenario in

the area. The results show that from 10 June to 16 June, there were positive EHF values. The results in Table 1 depict that there is a heatwave-like scenario in the study region. The heatwaves are characterized using EHF severity levels (EHF_{sev}) as (Varghese et al., 2019)

- No heatwave: daily EHF_{sev} ≤ 0
- Low severity: daily EHF_{sev} > 0 and < 1
- Moderate severity: daily EHF_{sev} ≥ 1 and < 2
- High severity: daily EHF_{sev} ≥ 2

Figure 3 shows the variation of these indices and the variation in mean temperature. However, there were more days of EHF_{sev} ≥ 2 during the study period. A similar range of values and slightly higher values of EHF are also reported in a study conducted over various cities globally. It includes the cities of Adelaide, Melbourne, London, Chicago, Paris, Moscow, and Guangzhou (Nairn et al., 2018).

Table 1 Days with positive EHF values and their level of severity

Date	EHI _{sig}	EHI _{accl}	EHF	Level of severity
10-06-2023	0.152967	2.831252	0.433087	Low
11-06-2023	0.693367	3.214097	2.228547	High
12-06-2023	1.152383	3.561843	4.104609	High
13-06-2023	1.409733	3.743575	5.277442	High
14-06-2023	0.994267	3.214733	3.196302	High
15-06-2023	0.717983	2.842147	2.040614	High
16-06-2023	0.44595	2.481868	1.106789	Moderate

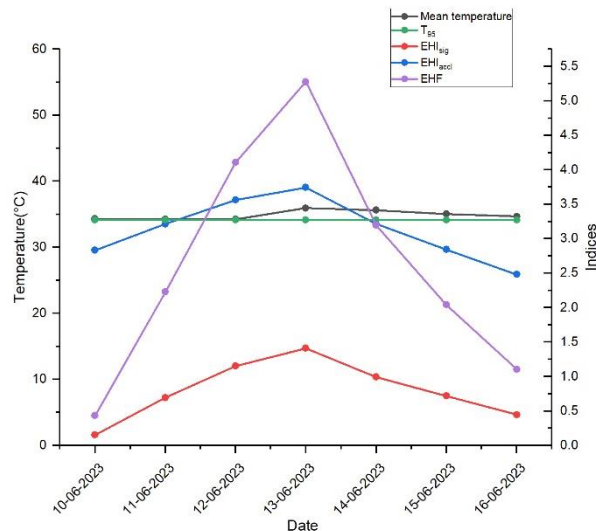


Figure 3. Schematic representation of a short duration heatwave in the summer season. The DMT and 95th percentile (both in $^{\circ}\text{C}$) are plotted against the left-hand axis, while the three heatwave indices (in $^{\circ}\text{C}$) are plotted against the right-hand axis.

4.2 Variability in daytime UHI intensity for pre, post and during heatwave days

The variability in UHI intensity during pre, post, and during heatwave is observed in the region during the heatwave event of June 2023 based on positive EHF values. Figure 4 shows the spatio-temporal variation of UHI intensities during daytime for pre, post and during heatwave days. The variations show that the area is consistently warmer, especially the main urban cluster. The northeastern portion of the region is cooler as

compared to urban areas for the pre heatwave days 07, 08 and 10 June 2023. This variation starts developing more in the northeastern part when the heatwave event starts and reaches the southwestern part on 14 June 2023. The variations start minimizing, and the colder areas start developing again after the heatwave event.

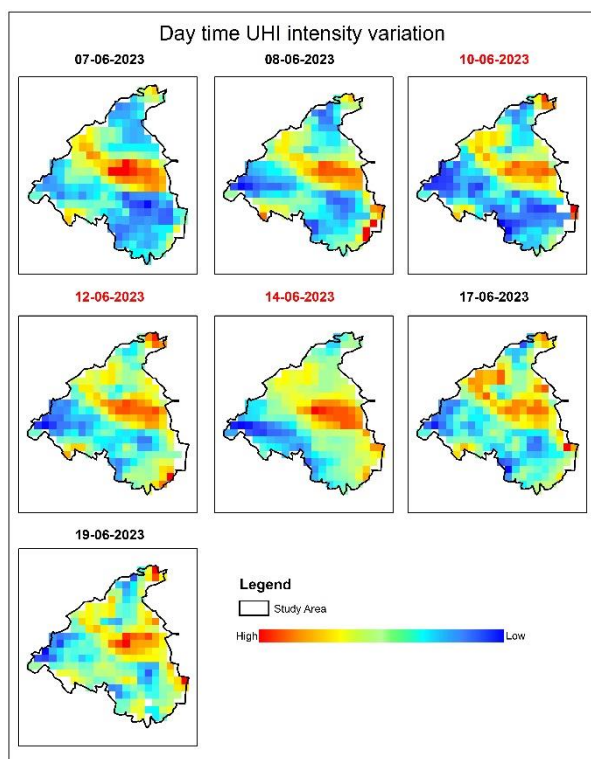


Figure 4. Variability of daytime UHI intensity for pre, post and during heatwave events in the area (Dates highlighted with red colour are heatwave days)

There is a distinctive temperature distribution during the heatwave compared to those during the pre and post heatwave periods. During the pre-heatwave period, most areas had temperatures lower than 40 °C, whereas during the heatwave, almost the entire region (except the northwestern part) had high temperatures above 41 °C. During the post-heatwave period, only the southeastern part of the area experiences high temperatures.

4.3 Variability in nighttime UHI intensity for pre, post and during heatwave days

The variability in UHI intensity during pre, post, and during heatwave is observed in the region during the heatwave event of June 2023 based on positive EHF values. Figure 5 shows the spatio-temporal variation of UHI intensities during nighttime for pre, post and during heatwave days. The variations show that the area is consistently cooler except for the warmer urban cluster. The surrounding portion of the region is cooler compared to urban areas for the pre heatwave days 07, 08 and 10 June 2023. This variation starts developing as the heatwave event starts, and the night temperatures are rising more in the northwestern part on the night of 13 June 2023. The variations start minimizing, and the colder areas start developing again after the heatwave event.

There is a distinctive temperature distribution at nighttime during the heatwave compared to those during the pre and post heatwave periods. During the pre-heatwave period, most areas

had temperatures of about 29 °C, whereas during the heatwave, almost the entire region (except the northwestern part) had high temperatures above 30 °C. During the post-heatwave period, only the southeastern part of the area experiences high temperatures.

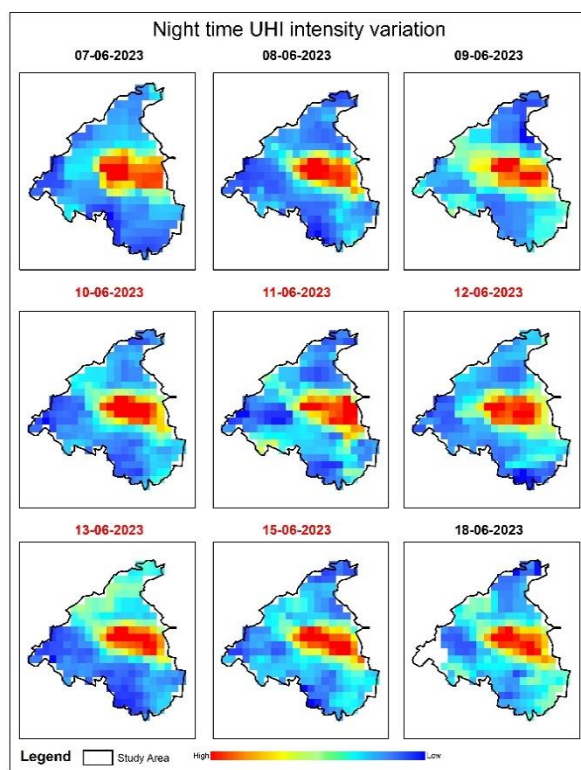


Figure 5. Variability of nighttime UHI intensity for pre, post and during heatwave event in the area (Dates highlighted with red colour are heatwave days)

4.4 Daytime and nighttime variation of temperatures for pre, post and during heatwave days

Figure 6 shows the variation of maximum, minimum, and mean diurnal temperatures during daytime for pre, post and during heatwave days. The difference in the maximum and minimum temperature in the pre heatwave period is about 6-7 °C. This difference is amplified during the heatwave period and has a difference of 8-9 °C. As the heatwave period ends, the temperature difference is like pre heatwave period, which is in the range of 6-7 °C. This indicates the difference in the maximum and minimum temperatures from pre heatwave period to heatwave period and heatwave period to post heatwave period is 2 °C.

Similarly, the difference in the maximum and mean temperatures is also observed. The difference in the maximum and mean temperature in the pre heatwave period is about 4-5 °C. This difference is amplified during the heatwave period and has a difference of 5-6 °C. As the heatwave period ends, the temperature difference is like pre heatwave period which is in the range of 5-6 °C. This indicates the difference in the maximum and mean temperatures from pre heatwave period to heatwave period and heatwave period to post heatwave period it is of 1 °C. This indicated significantly elevated temperatures and increased heat stress during the daytime. This trend of elevated daytime temperatures is also seen during heatwaves i.e., by 1-2°C in other studies based upon the simulated results or station data (Rizvi et al., 2019).

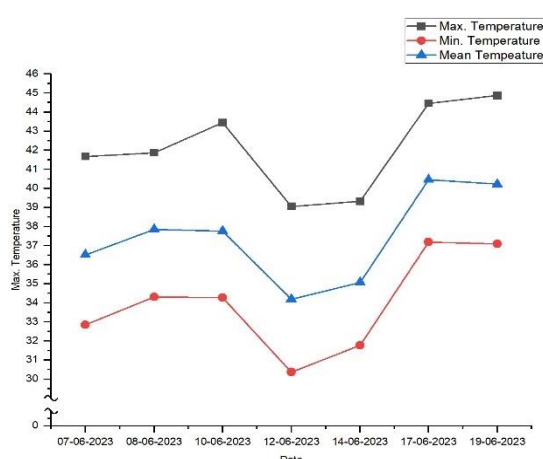


Figure 6. Variability of daytime temperature for pre, post and during heatwave event in the area

Figure 7 shows the variation of maximum, minimum, and mean diurnal temperatures during nighttime for pre, post, and during heatwave days. The difference in the maximum and minimum temperature in the pre heatwave period is about 4-7 °C. This difference is kept the same during the heatwave period with a difference of 4-7 °C. As the heatwave period ends, the temperature difference is like pre heatwave period, which is in the range of 6-7 °C. This indicated that the difference in the maximum and minimum temperatures from pre heatwave period to heatwave period and heatwave period to post heatwave period is consistent with no significant changes in the temperature.

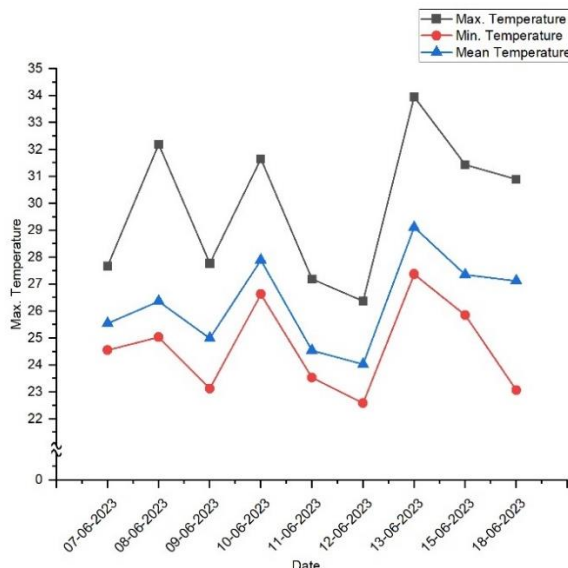


Figure 7. Variability of nighttime temperature for pre, post and during heatwave event in the area

Similarly, the difference in the maximum and mean temperatures is also observed. The difference in the maximum and mean temperature in the pre heatwave period is about 3-6 °C. This difference is reduced during the heatwave period and has a difference of 4-6 °C. As the heatwave period ends, the temperature difference is like pre heatwave period which is in the range of 4-6 °C. This indicated that the difference in the maximum and mean temperatures from pre heatwave period to

heatwave period and heatwave period to post heatwave period is consistent with no significant changes in the temperature. This indicates that there are no significant elevated temperatures during the nighttime during a heatwave scenario. This trend of elevated daytime temperatures is also seen during heatwaves i.e., by 1 °C or less in other studies based upon the station data (Richard et al., 2021)

4.5 Validation of UHI intensity for pre, post and during heatwave days

The magnitude of UHI intensity is estimated for the heatwave days when there were positive EHF values. These UHI intensity values are also calculated using ERA-5 Land hourly data. The hourly data is averaged and the daily mean is calculated for pre and post-days of heatwave event in the area. The results have shown a sudden increase in the UHI intensity values can be seen from one day before the actual heatwave event occurred and this impact was prolonged till one day after the heatwave event in the region. Figure 8 depicts the variation of EHF values and UHI intensity on the gridded location of a weather station at 29.5° N, 79.5° E.

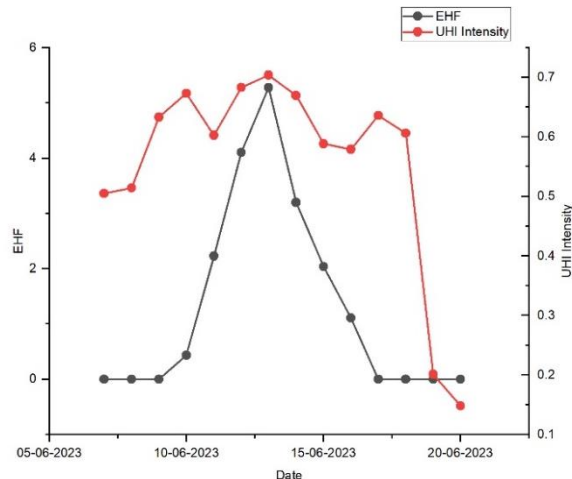


Figure 8. Variation of UHI intensity and EHF values during heatwave event of 10-16 June 2023. EHF values are plotted against the left-hand axis, while the UHI intensity is plotted against the right-hand axis. The T_{95} value at this site is 34.12 °C

5. Conclusion

The results validate the intensification of UHI intensity during the heatwave event in the area as compared to pre and post days intensity values. The results show that there is a heatwave event in the area from 10-16 June 2023 with positive EHF values. The values range from 0.433087-5.277442 during the event. The daytime and nighttime variation of maximum, minimum and mean temperatures establish that there is an amplification of temperature between pre, post and during heatwave days in daytime variation, which is 2 °C whereas this variation is constant in nighttime.

The results are validated using ERA-5 Land data, and the UHI intensities are calculated during pre, post, and during heatwave. The UHI intensity ranges between 0.504764 – 0.633209 during pre-heatwave event. The intensity value kept on increasing as the heatwave event approached reached the maximum magnitude of 0.70384 during the heatwave event. As the event finishes, intensity values decrease to 0.147939 post heatwave event. The findings of this study depicted that UHI intensity

was directly impacted during the heatwave event. The future scope of this study aims to analyze the other responsible factors like precipitation, wind speed, energy fluxes, and others that can help investigate extreme events. The EHF could be used in future studies across different climates to evaluate the adaptability of the EHF in various locations, especially with higher humidity.

References

Arellano, B., Roca, J., 2022. Effects of urban greenery on health. a study from remote sensing, *Int. Arch. Photogramm. Remote Sens. Spat. Inf. Sci. - ISPRS Arch.* pp. 17–24. <https://doi.org/10.5194/isprs-archives-XLIII-B3-2022-17-2022>

Census. 2011. *Census of India 2011* Farrukhabad. <https://doi.org/10.4324/9781003476900-33>

Goyal, M.K., Singh, S., Jain, V., 2023. Heat waves characteristics intensification across Indian smart cities. *Sci. Rep.* 13, 1–16. <https://doi.org/10.1038/s41598-023-41968-8>

H.-O. Pörtner, D.C. Roberts, M. Tignor, E.S. Poloczanska, K. Mintenbeck, A. Alegría, M. Craig, S. Langsdorf, S. Löschke, V. Möller, A. Okem, B.R., 2021. IPCC, 2022, *Clim. Chang. 2022 Impacts, Adapt. Vulnerability. Contrib. Work. Gr. II to Sixth Assess. Rep. Intergov. Panel Clim. Chang.* <https://doi.org/10.1017/9781009325844>

Hatvani-Kovacs, G., Belusko, M., Pockett, J., Boland, J., 2016. Can the excess heat factor indicate heatwave-related morbidity? A case study in Adelaide, South Australia. *Ecohealth* 13, 100–110. <https://doi.org/10.1007/s10393-015-1085-5>

He, B.J., Wang, J., Liu, H., Ulpiani, G., 2021. Localized synergies between heat waves and urban heat islands: Implications on human thermal comfort and urban heat management. *Environ. Res.* 193. <https://doi.org/10.1016/j.envres.2020.110584>

Mamgain, S., Gupta, K., Roy, A., Karnataka, H.C., Singh, R.P., 2023. Long-term thermal anomaly detection and mapping at pixel level using a Google Earth Engine tool. *Int. Arch. Photogramm. Remote Sens. Spat. Inf. Sci. - ISPRS Arch.* 48, 147–153. <https://doi.org/10.5194/isprs-archives-XLVIII-M-3-2023-147-2023>

Nairn, J., Fawcett, R., 2013. Defining heatwaves: Heatwave defined as a heat-impact event servicing all community and business sectors in Australia, *CAWCR technical report*

Nairn, J., Ostendorf, B., Bi, P., 2018. Performance of excess heat factor severity as a global heatwave health impact index. *Int. J. Environ. Res. Public Health* 15. <https://doi.org/10.3390/ijerph15112494>

Nairn, J.R., Fawcett, R.J.B., 2014. The excess heat factor: A metric for heatwave intensity and its use in classifying heatwave severity. *Int. J. Environ. Res. Public Health* 12, 227–253. <https://doi.org/10.3390/ijerph120100227>

Rao, K.K., Jyoteshkumar Reddy, P., Chowdary, J.S., 2023. Indian heatwaves in a future climate with varying hazard thresholds. *Environ. Res. Clim.* 2, 015002. <https://doi.org/10.1088/2752-5295/acb077>

Richard, Y., Pohl, B., Rega, M., Pergaud, J., Thevenin, T., Emery, J., Dudek, J., Vairet, T., Zito, S., Chateau-Smith, C., 2021. Is Urban Heat Island intensity higher during hot spells and heat waves (Dijon, France, 2014–2019)? *Urban Clim.* 35. <https://doi.org/10.1016/j.uclim.2020.00747>

Rizvi, S.H., Alam, K., Iqbal, M.J., 2019. Spatio -temporal variations in urban heat island and its interaction with heat wave. *J. Atmos. Solar-Terrestrial Phys.* 185, 50–57. <https://doi.org/10.1016/j.jastp.2019.02.001>

Rohini, P., Rajeevan, M., Srivastava, A.K., 2016. On the Variability and Increasing Trends of Heat Waves over India. *Sci. Rep.* 6, 1–9. <https://doi.org/10.1038/srep26153>

Scalley, B.D., Spicer, T., Jian, L., Xiao, J., Nairn, J., Robertson, A., Weeramanthri, T., 2015. Responding to heatwave intensity: Excess Heat Factor is a superior predictor of health service utilisation and a trigger for heatwave plans. *Aust. N. Z. J. Public Health* 39, 582–587. <https://doi.org/10.1111/1753-6405.12421>

Sy, I., Cissé, B., Ndao, B., Touré, M., Diouf, A.A., Sarr, M.A., Ndiaye, O., Ndiaye, Y., Badiane, D., Lalou, R., Janicot, S., Ndione, J.A., 2022. Heat waves and health risks in the northern part of Senegal: analysing the distribution of temperature-related diseases and associated risk factors. *Environ. Sci. Pollut. Res.* 29, 83365–83377. <https://doi.org/10.1007/s11356-022-21205-x>

Tan, J., Zheng, Y., Tang, X., Guo, C., Li, L., Song, G., Zhen, X., Yuan, D., Kalkstein, A.J., Li, F., Chen, H., 2010. The urban heat island and its impact on heat waves and human health in Shanghai. *Int. J. Biometeorol.* 54, 75–84. <https://doi.org/10.1007/s00484-009-0256-x>

UN Habitat, 2022. Envisaging the Future of Cities, *World City Rep.* 2022.

Urban, A., Hanzlíková, H., Kyselý, J., Plavcová, E., 2017. Impacts of the 2015 heat waves on mortality in the Czech Republic-A comparison with previous heat waves. *Int. J. Environ. Res. Public Health* 14, 1–19. <https://doi.org/10.3390/ijerph14121562>

Varghese, B.M., Barnett, A.G., Hansen, A.L., Bi, P., Nairn, J., Rowett, S., Nitschke, M., Hanson-Easey, S., Heyworth, J.S., Sim, M.R., Pisaniello, D.L., 2019. Characterising the impact of heatwaves on work-related injuries and illnesses in three Australian cities using a standard heatwave definition- Excess Heat Factor (EHF). *J. Expo. Sci. Environ. Epidemiol.* 29, 821–830. <https://doi.org/10.1038/s41370-019-0138-1>

Wang, Y., Nordio, F., Nairn, J., Zanobetti, A., Schwartz, J.D., 2018. Accounting for adaptation and intensity in projecting heat wave-related mortality. *Environ. Res.* 161, 464–471. <https://doi.org/10.1016/j.envres.2017.11.049>

Xu, Z., Fitzgerald, G., Guo, Y., Jalaludin, B., Tong, S., 2016. Impact of heatwave on mortality under different heatwave definitions: A systematic review and meta-analysis. *Environ. Int.* <https://doi.org/10.1016/j.envint.2016.02.007>

Zachariah, M., T, A., AchutaRao, K., Saeed, F., Jha, R., Dhasmana, M.K., Mondal, A., Bonnet, R., Vautard, R., Philip, S., Kew, S., Vahlberg, M., Singh, R., Arrighi, J., Heinrich, D., Thalheimer, L., Marghidian, C.P., Kapoor, A., van Aelst, M., Raju, E., Li, S., Sun, J., Vecchi, G., Yang, W., Hauser, M., Schumacher, D.L., Senaviratne, S.I., Harrington, L.J., Otto, F.E., 2022. Climate Change made devastating early heat in India and Pakistan 30 times more likely. *World Weather Attrib.* 43.

Zhang, A., Wang, Q., Yang, X., Liu, Yuanyuan, He, J., Shan, A., Sun, N., Liu, Q., Yao, B., Liang, F., Yang, Z., Yan, X., Bo, S., Liu, Yang, Mao, H., Chen, X., Tang, N. jun, Yan, H., 2023. Impacts of heatwaves and cold spells on glaucoma in rural China: A national cross-sectional study. *Environ. Sci. Pollut. Res.* 30, 47248–47261. <https://doi.org/10.1007/s11356-023-25591-8>